Available online at www.sciencedirect.com
SCIENCE DIRECT®
Journal of Chromatography A, 1018 (2003) 137–153
JOURNAL OF CHROMATOGRAPHY A
www.elsevier.com/locate/chroma

Effect of salts and temperature on the adsorption of bovine serum albumin on polypropylene glycol-Sepharose under linear and overloaded chromatographic conditions☆

A.C. Dias-Cabral[a], J.A. Queiroz[a], N.G. Pinto[b,*]

[a] *Department of Chemistry, University of Beira Interior, 6201-001 Covilhã, Portugal*
[b] *Department of Chemical and Materials Engineering, University of Cincinnati, Cincinnati, OH 45221-0171, USA*

Received 1 November 2002; received in revised form 25 June 2003; accepted 2 July 2003

Abstract

The interaction thermodynamics associated with bovine serum albumin (BSA) adsorption on polypropylene glycol (PPG)-Sepharose CL-6B gel, using ammonium and sodium sulfate was studied. Analysis of data under linear conditions was accomplished with the stoichiometric displacement retention model and preferential interaction approach. Preferential interaction analysis indicated a strong entropic driving force due to the release of a large amount of solvent on adsorption. Flow microcalorimetry provided direct heat of adsorption measurements under overloaded conditions and confirmed that the adsorption of BSA on PPG-Sepharose was entropically driven within the range of conditions studied. Using these data in combination with isotherm measurements, it is shown that protein surface coverage, salt concentration, salt type and temperature affect the enthalpic and entropic behavior in hydrophobic interaction chromatography (HIC). This study shows that protein–sorbent interactions can be strongly influenced by the degree of water release, protein–protein interactions on the surface, and the re-orientation and/or reconfiguration of the adsorbed protein.

Keywords: Hydrophobic interaction chromatography; Adsorption; Polypropylene glycol-Sepharose; Thermodynamic parameters; Salt effects; Temperature effects; Calorimetry; Albumin; Proteins

1. Introduction

Hydrophobic interaction chromatography (HIC) is a very popular methodology used in the purification of biomolecules. Reports in the literature include the removal of viruses from human plasma, the successful isolation of bacterial enzymes, and the purification of therapeutic proteins and monoclonal antibodies [1–5]. Recently this technique has also been used to purify plasmids for gene therapy applications [6].

HIC is a very powerful adsorptive separation technique for several reasons. Separations are achieved quickly, with little product degradation and low solvent requirements, with very good levels of purification [1]. The selectivity of HIC changes with the temperature and hydrophobicity of the column and with the composition of the mobile phase. A better

☆ Presented at the International Symposium on Preparative and Industrial Chromatography and Allied Techniques, Heidelberg, 6–9 October 2000.

* Corresponding author. Tel.: +1-513-556-2761; fax: +1-513-556-3473.
E-mail address: neville.pinto@uc.edu (N.G. Pinto).

0021-9673/$ – see front matter © 2003 Elsevier B.V. All rights reserved.
doi:10.1016/j.chroma.2003.07.010

understanding of the influences of these factors is essential to quantify the mechanisms that establish equilibrium characteristics such as capacity and selectivity. A number of models [7–10] have been proposed, with limited success. This is mainly because of non-idealities originating from intermolecular interactions are not satisfactorily described, particularly under overloaded conditions [11].

Geng et al. [10] proposed the stoichiometric displacement retention model for the HIC of proteins. This model is based on their conclusion that no matter how different the interactions between adsorbent and solute or solvent molecules are, or how heterogeneous the distribution of these active sites is, a rational mechanism for adsorption in a liquid–solid system should be stoichiometric displacement for solute adsorption [12]. The model, when applied to linear chromatography, reduces to:

$$\ln k' = \ln I - Z \ln[\mathrm{H_2O}] \tag{1}$$

where

$$I = K[L_\mathrm{d}]^{n'}\phi \tag{2}$$

and

$$Z = Z_{\mathrm{H_2O}} - Z_\mathrm{s} \tag{3}$$

Z denotes the number of water molecules released per protein molecule adsorbed, $Z_{\mathrm{H_2O}}$ is the Z value with water as the mobile phase, and Z_s the change in the number of water molecules released as protein molecules are transferred from water into an aqueous salt solution. The intercept of this equation, $\ln I$, contains a number of constants. K is the equilibrium constant, L_d corresponds to the hydrated ligands in salt solution, n' the number of ligand interactions with a protein molecule and ϕ the column phase ratio. When the salt, ligand and temperature are fixed, Z is a characteristic constant related to protein conformation [10].

Karger and co-workers [9] used a plot $\ln k'$ versus the concentration of water (%B, volume fraction) to characterize protein adsorption in HIC. They were exploring methods for recognizing protein conformational changes that can occur as a function of temperature. They demonstrated that the slope of the plot $[\partial(\ln k')/\partial(\ln \%B)]$ is a sensitive measure of protein conformation, which is related with the contact area of the adsorbed protein on the surface [9]. The relationship between the equation of Karger and co-workers and Eq. (1) has been discussed in the Appendix A. It is shown that $[\partial(\ln k')/\partial(\ln \%B)]$ and Z are directly related. Thus Z is also a measure of the conformation of the protein on the adsorbent surface.

The equation developed by Perkins et al., like that of Karger and co-workers is based on the preferential interaction theory [8], and is:

$$\ln k' = C + \frac{\Delta\nu_+ + \Delta\nu_-}{g}\ln m_3 - \frac{n\,\Delta\nu_1}{m_1 g}m_3 \tag{4}$$

where m is molal concentration. The subscripts 1 and 3 refer to the solvent and solute, respectively. $\Delta\nu_i$ is the stoichiometrically weighted change in the number of species in the local region of products and reactants of the process and n the total number of anions $(-)$ and cations $(+)$ associated with the electrolyte. g is the ratio of $(\partial \ln m_3/\partial \ln a_3)_{T,P}$, where a is the activity of the modulator (a discussion on calculating g can be found in [8]), and C the integration constant. From Eq. (4), the change in the binding of ions $(\Delta\nu_+ + \Delta\nu_-)$ and the number of water molecules released $(\Delta\nu_1)$ can be estimated. The relationship between Eqs. (4) and (1) has been discussed in the Appendix A.

All of the models discussed above are applicable only to linear chromatography. For the overloaded region, the commonly used approach is to characterize behavior with isotherm measurements at a limited set of conditions [11]. The experimental isotherms are fitted to empirical models, such as the Langmuir or bi-Langmuir. While this approach is relatively direct and convenient, it is nonetheless risky [11]. Since the isotherm parameters are not linked fundamentally to underlying mechanisms, interpolation or extrapolation can lead to erroneous predictions [11,15,16]. In an effort to overcome this problem, our group [11,17–19] has turned to calorimetry. This technique provides valuable data on the overall enthalpy change of adsorption (ΔH_ads) in the non-linear region of the isotherm.

This paper presents experimental data from equilibrium binding isotherms, linear chromatography, and calorimetry, obtained to examine the thermodynamics of bovine serum albumin (BSA) adsorption on polypropylene glycol (PPG)-Sepharose CL-6B gel at various salt conditions and temperatures. Analyses in the linear region of the isotherm were made with the stoichiometric displacement retention model and preferential interaction analysis. The non-linear region was characterized with isotherm measurements

and calorimetry. All of these data were used to gain insight on the complex HIC adsorption process.

2. Experimental

2.1. Materials and methods

The HIC support used (Fig. 1) is a Sepharose derivative synthesized by covalent immobilization of polypropylene glycol on Sepharose CL-6B according to Sundberg and Porath [20]. The synthesis procedure has been described in detail elsewhere [21]. Briefly, PPG-diglycidyl-ether (average number–average molecular mass, M_n, ca. 380) from Aldrich (Steinheim, Germany) is coupled to Sepharose CL-6B (Amersham Biosciences, Uppsala, Sweden) in the presence of a solution of sodium hydroxide and sodium borohydride, both from Merck (Darmstadt, Germany). The derivatized gel is then treated with a solution of sodium hydroxide overnight at room temperature to inactivate free epoxy groups. The derivatized gel wet bead size ranges between 45 and 165 μm.

The probe protein BSA was purchased from Sigma (St. Louis, MO, USA), and used without further purification. BSA is a globular ellipsoid (14 nm × 4 nm × 4 nm), with a molecular mass of approximately 69 000 Da, and an isoelectric point of 4.7 [22].

A 10 mM sodium phosphate buffer, which consisted of a mixture of solutions of dibasic and monobasic sodium phosphate from Aldrich (Steinheim, Germany), was used for all the experiments. Analytical-grade ammonium sulfate and sodium sulfate from Aldrich (Steinheim, Germany) were used as modulators.

2.2. Flow microcalorimetry

The heat of adsorption was measured using a Flow MicroCalorimeter (FMC) (Gilson Instruments, Westerville, OH, USA). The FMC operates isothermally, and has a precision fluid delivery system (syringe micropumps), a vacuum system to pre-evacuate a sample in situ, and a block heater and monitor to control cell temperature. Interfaced with the cell are two highly sensitive thermisters. These are capable of detecting small temperature changes within the cell that are associated with the adsorption of an analyte onto the surface of a particular adsorbent. Calibration is by electrical energy dissipation in the cell under static or flowing conditions.

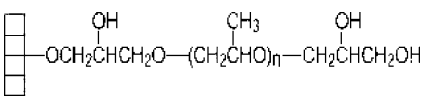

Fig. 1. Structure of PPG-Sepharose ($n = 3$).

The FMC is operated similar to a liquid chromatograph with the cell (0.171 ml) in place of the column, and is equipped with a configurable injection loop to accommodate different injection volumes. The effluent was collected and analyzed with a UV spectrophotometer (Milton Roy, Rochester, NY, USA) at a wavelength of 280 nm.

The FMC cell is packed with a specified amount of the dried support, depending on its swelling characteristics. Deionized (DI) water is then introduced until equilibration; this wetting process takes at least 48 h. Following equilibration, the syringe pumps are turned on and the adsorbent is equilibrated first with the buffered solution and then with the carrier solution at a flow-rate of 3.33 ml h^{-1}. Once the system has reached thermal equilibrium, the protein sample is loaded into an injection loop (0.128 ml for sodium sulfate as modulator and 0.323 ml for ammonium sulfate) and introduced into the cell by switching a multiport valve. The adsorption of the sample onto an adsorbent surface causes a change in cell temperature, which is converted to a heat signal by the FMC through an experimentally determined calibration factor (the calibration factor was obtained using an electrical impulse of 0.030 J). Once the mass in the effluent is quantified with the spectrophotometer, a simple mass balance is performed to determine the quantity of sample adsorbed. The specific heat of adsorption is calculated from these data.

The heats of adsorption measurements of BSA on PPG-Sepharose were performed at selected concentrations of ammonium sulfate and sodium sulfate at various temperatures, and with a range of BSA concentrations between 20 and 60 mg ml^{-1}.

2.3. Isotherms

BSA adsorption isotherms were measured at selected modulator concentrations and temperatures

using a batch method. Dried PPG-Sepharose was first weighed into politops, and then a measured volume of protein solution of a known salt and protein concentration at pH 7 was added. The politops were then placed in an orbital shaker (ARALAB, Oeiras, Portugal) maintained at the selected temperature and agitated at 230 rpm for 24 h. Preliminary experiments established that equilibrium is reached in 8–10 h. After equilibration, the slurry solution was allowed to settle for 30 min and a sample of the supernatant was removed with a filter (0.45 μm) syringe. The absorbance of the filtrate was measured at 280 nm, with a UV spectrophotometer (Amersham Biosciences, Uppsala, Sweden), to obtain the equilibrium solution concentration. The equilibrium distribution was calculated from a mass balance.

2.4. Isocratic elutions

The capacity factor measurements for BSA were carried out at different temperatures in a fast protein liquid chromatography (FPLC) system (Amersham Biosciences, Uppsala, Sweden). The gel was packed in a column (4.2 cm × 1.0 cm i.d.) and equilibrated with the desired mobile phase at a flow-rate of 0.24 ml min^{-1}. Elution times (t_r) were obtained by injecting 100 μl of 2.00 ± 0.02 mg ml^{-1} BSA. The elution profile was determinate by continuous measurements of the absorbance at 280 nm. Following the elution, the column was washed with the 10 mM phosphate buffer (pH 7).

3. Results and discussion

3.1. Linear region

The retention behavior of BSA on the PPG-Sepharose column was investigated as a function of salt type, salt concentration and temperature.

Isocratic elutions of BSA on PPG-Sepharose, carried out with ammonium sulfate and sodium sulfate at 296.15 K showed that protein retention increases with increasing salt concentration in the mobile phase. This trend was observed at all temperatures. The presence of salt has a great influence on the equilibrium behavior in HIC [1]. The free energy of a protein in solution is increased in presence of either ammonium sulfate or sodium sulfate, due to the water-structuring characteristic of these salts. The interaction between protein and salt increase as the salt concentration is increased. Salt molecules displace some of the water molecules surrounding the protein, and the protein in an effort to reduce its free energy adsorbs on the gel surface. This, in effect, reduces the free energy of the protein because the protein surface area exposed to the salt is reduced [7].

Higher retention of protein was observed in the presence of Na_2SO_4 compared to $(NH_4)_2SO_4$ for each concentration, indicating that sodium sulfate has a greater ability to enhance hydrophobic interactions between BSA and PPG-Sepharose [4]. This observation is consistent with previously reported data, documenting that Na_2SO_4 has a larger molal surface tension increment than $(NH_4)_2SO_4$ (2.73×10^{-3} dyn g cm^{-1} mol^{-1} versus 2.16×10^{-3} dyn g cm^{-1} mol^{-1}, respectively [7,23]). The greater ability for water-structuring manifests as a greater surface tension enhancement, which strengths the protein–ligand interaction [24,25].

The retention factor, k', measured under isocratic conditions was evaluated directly from the chromatogram as [26]:

$$k' = \frac{t_r - t_0}{t_0} \quad (5)$$

where t_r is the solute retention time and t_0 the elution dead time (measured with an inert tracer). As shown in Fig. 2a and b, k' increases with an increase in temperature, as is generally observed for HIC [27], and the dependence of k' on temperature increases when the concentration of salt increases from 0.8 to 1.5 M for ammonium sulfate and 0.8 to 1.2 M for sodium sulfate. Generally, the capacity factor does not change linearly with temperature, and, if it does, it is over a very small range. The non-linearity is, in part [28], due to a change in protein conformation, which results in an increase in the conformational entropy at higher temperature.

It is well know that a protein in a folded state is less retained in HIC than in an unfolded state [9,29–31]. This is because the area of contact of the protein with the adsorbent surface is generally larger in an unfolded state. Thus, a non-linear dependence of retention with temperature could be due to a conformational change in the protein [9].

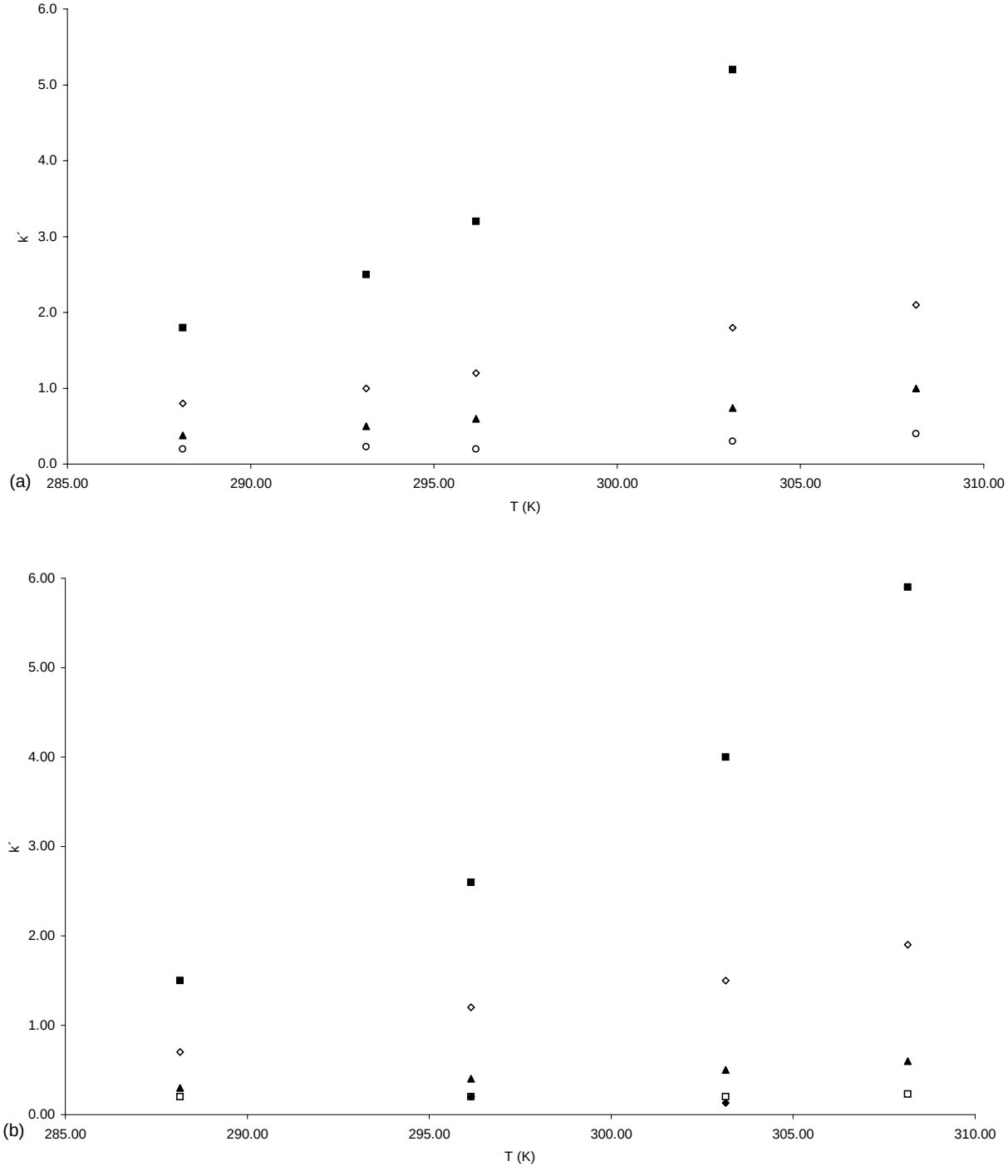

Fig. 2. (a) Plots of k' vs. temperature for BSA adsorption on PPG-Sepharose using as modulator Na_2SO_4 at pH 7((○) 0.80 M; (▲) 1.00 M; (◇) 1.10 M; (■) 1.20 M). (b) Plots of k' vs. temperature for BSA adsorption on PPG-Sepharose using as modulator $(NH_4)_2SO_4$ at pH 7 ((◆) 0.80 M; (□) 1.00 M; (▲) 1.20 M; (◇) 1.40 M; (■) 1.50 M).

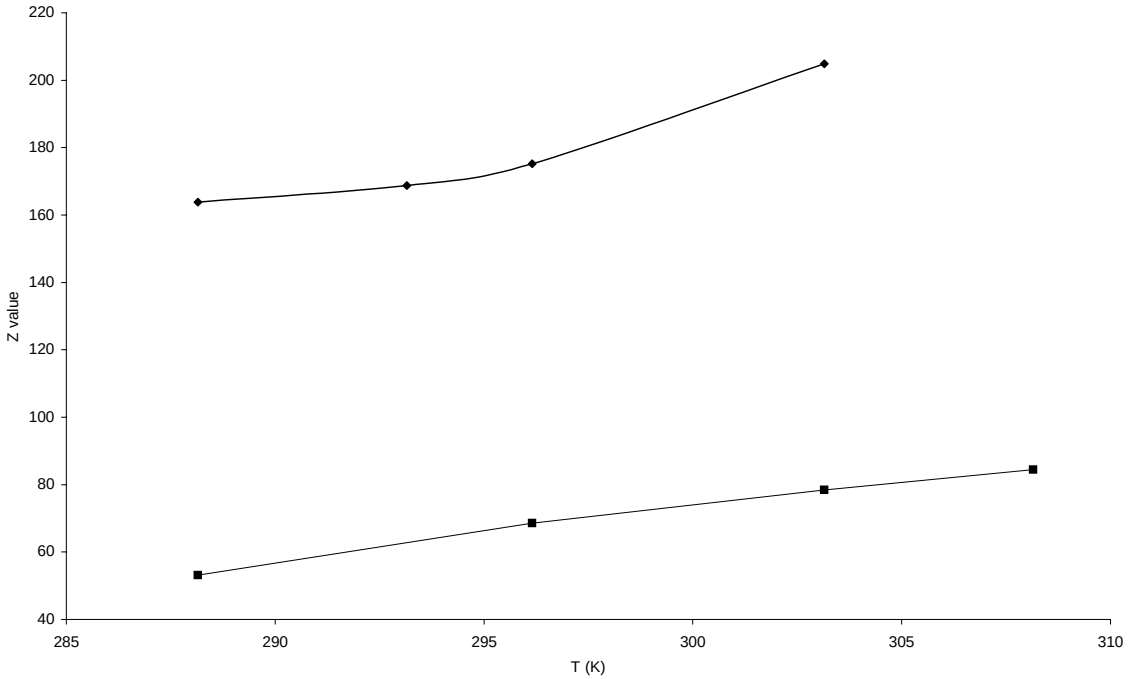

Fig. 3. Plot of Z values of BSA vs. temperature using as modulator (◆) Na_2SO_4 and (■) $(NH_4)_2SO_4$.

An important measurement, one that can reflect changes in contact area, is the change of protein retention with solvent composition. Capacity factors can be analyzed with Eq. (1), to obtain Z which is a measure of protein conformation. Fig. 3 shows the change in Z value as function of column temperature. Only salt concentrations higher than 0.80 M were used; this is because of the small retention of the protein on the support surface at 0.80 M. For both salts, the Z value increases with temperature. For sodium sulfate, there is a sharp change in the Z value at approximately 295 K, indicating a conformational change in the protein [9]. In contrast, with ammonium sulfate no sharp change is evident.

HIC retention data of BSA on PPG-Sepharose, for both ammonium sulfate and sodium sulfate, were graphed on a Van't Hoff plot ($\ln k'$ versus $1/T$) (Fig. 4). Following Haidacher et al.'s approach of incorporating the dependence of ΔH°, ΔS°, ϕ and ΔC_p^0 on temperature, the data in Fig. 4 were analyzed with the quadratic equation [27]. The best-fit coefficients obtained using Table Curve 2D, a non-linear least squares fitting program [32] that employs the Leventhal–Marquardt method, are summarized in Table 1; characterizations obtained with these coefficients are shown as solid curves in Fig. 4.

It can be seen in Table 1 that for both salts the process is predicted to be endothermic, indicating an entropically driven process, as is expected [8,9,33,34]. Exothermic values are observed at some low salt concentrations. This could be due to weaker hydrophobic interactions [8]. However, the trend is inconsistent in some cases. For example, for ammonium sulfate case 0.8 M, larger exothermic values are calculated at the higher temperatures where hydrophobic interactions are expected to be stronger.

It is also observed in Table 1 that for some concentrations of salt ΔH° increases as the temperature increases and for others it decreases. For example, for sodium sulfate, at 1.00 and 1.10 M ΔH° decreases with increasing temperature, while at 0.80 and 1.20 M it increases. Due to this, there are situations where at constant temperature the ΔH° can be larger at lower salt concentration. These observations are inconsistent with the expectation that the mechanism driving HIC shifts in the direction of a decreasing entropic

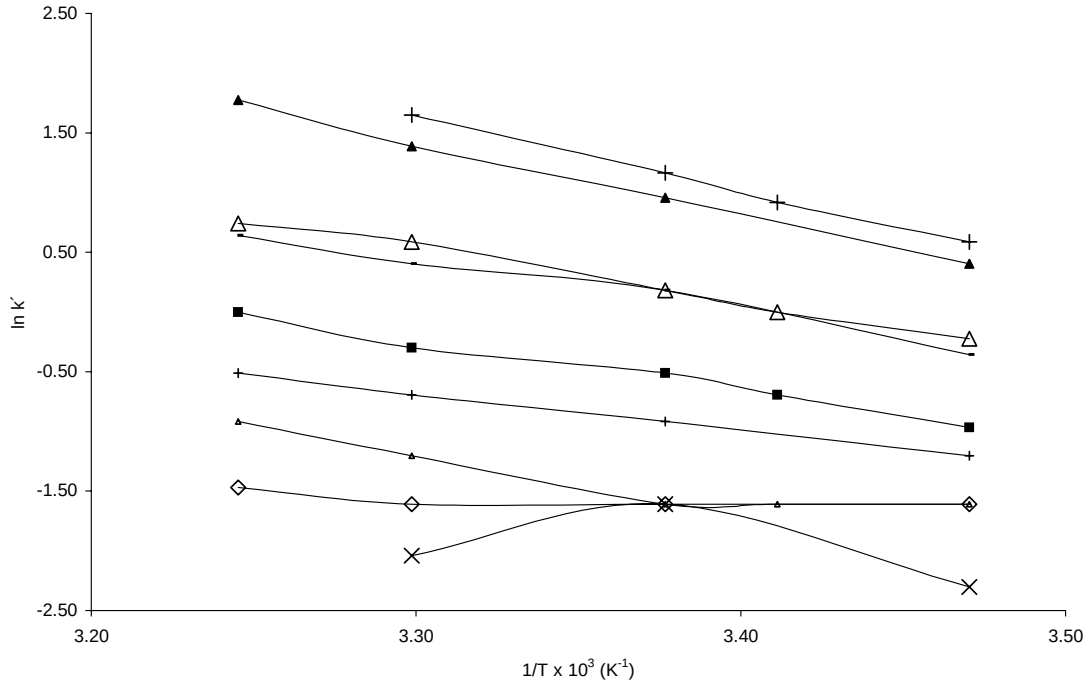

Fig. 4. Van't Hoff plots for the retention of BSA on PPG-Sepharose at different concentration of Na_2SO_4 and $(NH_4)_2SO_4$ at pH 7. The solid curves represent the quadratic equation adjusts ((▲) 0.80 M Na_2SO_4; (■) 1.00 M Na_2SO_4; (△) 1.10 M Na_2SO_4; (+) 1.20 M Na_2SO_4; (×) 0.80 M $(NH_4)_2SO_4$; (◇) 1.00 M $(NH_4)_2SO_4$; (+) 1.20 M $(NH_4)_2SO_4$; (−) 1.40 M $(NH_4)_2SO_4$; (▲) 1.50 M $(NH_4)_2SO_4$).

influence as the temperature is increased [8,26,27], and reinforces the conclusion reached earlier [17,18] that the thermodynamic values from the Van't Hoff analysis must be cautiously interpreted.

Because of the inconsistent temperature trends observed with the ΔH° and ΔS° values, no useful conclusions can be drawn by comparing these parameter values for the two salts. However, the standard Gibbs free energy, ΔG°, is always more negative for sodium sulfate, indicating that this salt is more effective in promoting adsorption of BSA on PPG-Sepharose. This is consistent with the retention order, and the molal surface tension increment imposed by each modulator [1,4,7,23,35].

The retention data were also analyzed with Eq. (4), derived from the preferential interaction analysis. With sodium sulfate as the modulator, the number of water molecules and salt ions released was calculated using $g = 1.64$ [8] and $n = 3$ and are shown in Table 2. The values with ammonium sulfate as the modulator were reported in an earlier publication [18], and have been repeated to facilitate comparisons. Since the anion is common for these modulators, the effect of the cation on water release can be investigated.

It is clear that for both modulators the adsorption is accompanied by the release of a large number of water molecules. It is also clear that the number of ions released is significant. While the release of a large number of water molecules is as expected, the substantial ion release may suggest some electrostatic influence. However, the stoichiometrically weighted change in the number of ions is generally similar for the two salts. Thus, the observed differences in protein retention for the two salts are most probably due to differences in the amount of water released. The results support the expectation of an entropically driven process, in which the release of a large number of ordered water molecules provides the driving force for adsorption.

The number of water molecules released is always greater for sodium sulfate (Table 2). This is consistent with the retention order. Preferential hy-

Table 1
Fit parameters of Van't Hoff analysis and thermodynamic quantities for the retention of BSA on PPG–Sepharose using as modulator $(NH_4)_2SO_4$ and Na_2SO_4 at pH 7

Temperature (K)	Concentration (M)	*a*	*b*	*c*	ΔH° (kcal mol^{-1})	ΔS° (cal mol^{-1}K^{-1})	ΔG° (kcal mol^{-1})
288.15	0.80 $(NH_4)_2SO_4$	−852.1	506023.3	−74978432	28.59	101.19	−0.56
296.15					0.66	5.55	−0.99
303.15					−22.57	−71.99	−0.75
308.15					−38.52	−124.17	−0.26
288.15	1.00 $(NH_4)_2SO_4$	78.3	−45137.1	6643728.4	−1.94	−3.41	−0.96
296.15					0.54	5.06	−0.96
303.15					2.59	11.94	−1.02
308.15					4.01	16.56	−1.10
288.15	1.20 $(NH_4)_2SO_4$	22.8	−9135.0	906667.4	5.65	23.61	−1.16
296.15					5.98	24.76	−1.35
303.15					6.27	25.70	−1.52
308.15					6.46	26.33	−1.66
288.15	1.40 $(NH_4)_2SO_4$	−66.4	45932.3	−7480714.5	11.9	47.09	−1.66
296.15					9.12	37.54	−2.00
303.15					6.80	29.81	−2.24
308.15					5.21	24.60	−2.37
288.15	1.50 $(NH_4)_2SO_4$	54.4	−23838.0	2661233.6	10.66	44.41	−2.13
296.15					11.66	47.80	−2.50
303.15					12.48	50.56	−2.84
308.15					13.05	52.41	−3.10
288.15					−1.40	−1.59	−0.96
293.15	0.80 Na_2SO_4	196.5	−112997.5	16381903	2.45	11.67	−0.97
296.15					4.70	19.30	−1.02
303.15					9.78	36.25	−1.21
308.15					13.26	47.65	−1.42
288.15					8.84	35.29	−1.32
293.15	1.00 Na_2SO_4	−0.3	5957.5	−1499607.3	8.49	34.08	−1.50
296.15					8.28	33.38	−1.60
303.15					7.82	31.83	−1.83
308.15					7.50	30.78	−1.98
288.15					9.34	38.38	−1.72
293.15	1.10 Na_2SO_4	6.9	2457.1	−1030929.1	9.09	37.55	−1.91
296.15					8.95	37.07	−2.02
303.15					8.63	36.00	−2.28
308.15					8.41	35.28	−2.46
288.15					11.33	46.95	−2.20
293.15	1.20 Na_2SO_4	58.9	−26029.2	2928506.8	12.02	49.32	−2.44
296.15					12.42	50.69	−2.59
303.15					13.33	53.72	−2.95
308.15					13.95	55.76	−3.23

dration is greater with Na^+ than NH_4^+. In the presence of sodium sulfate, the water structure around the protein and the adsorbent surface is more unstable, thus accounting for larger amounts of water release.

The results in Table 2 support the assumption made by Karger and co-workers that the salt term on the right hand side of Eq. (A.6) is negligible relative to the water term. However, on comparing the water release data given by Eq. (4) (Table 2) with that given

Table 2
Estimate of water molecules and salt ions released from adsorption of BSA on PPG-Sepharose using as modulator $(NH_4)_2SO_4$ and Na_2SO_4 at pH 7

Salt	Temperature (K)	$(n\,\Delta\nu_1)/(m_1/g)$ (kg mol^{-1})	$-(\Delta\nu_+ + \Delta\nu_-)/g$ (mol mol^{-1})	Regression correlation coefficient	$-\Delta\nu_1$ (mol mol^{-1})	$-(\Delta\nu_+ + \Delta\nu_-)$ (mol mol^{-1})
$(NH_4)_2SO_4$	288.15	7.70	5.47	0.9630	239	9
	296.15	15.01	14.19	1.0000	466	24
	303.15	13.16	10.82	0.9955	409	18
	308.15	18.04	16.89	0.9930	560	28
Na_2SO_4	288.15	24.57	19.72	0.9988	744	32
	293.15	24.35	19.13	0.9996	738	31
	296.15	20.44	14.32	0.9982	619	23
	303.15	29.56	23.30	0.9999	896	38
	308.15	21.28	15.66	1.0000	645	26

by Eq. (1) (Fig. 4), the values in Table 2, are consistently larger. This is a consequence of differences in the assumptions made by Wu et al. [9] and Perkins et al. [8], as outlined in detail in the Appendix A.

Concerning the number of water molecules/ions released as a function of temperature, for ammonium sulfate there is generally an increase with temperature, and for sodium sulfate, no distinct trend is observed.

3.2. Overloaded region

BSA isotherms on PPG-Sepharose measured at different concentrations of sodium sulfate (pH 7.0) at 303.15 K, are shown in Fig. 5. Also included in Fig. 5 are isotherms in the presence of ammonium sulfate. These were reported earlier [18], and have been included for convenience.

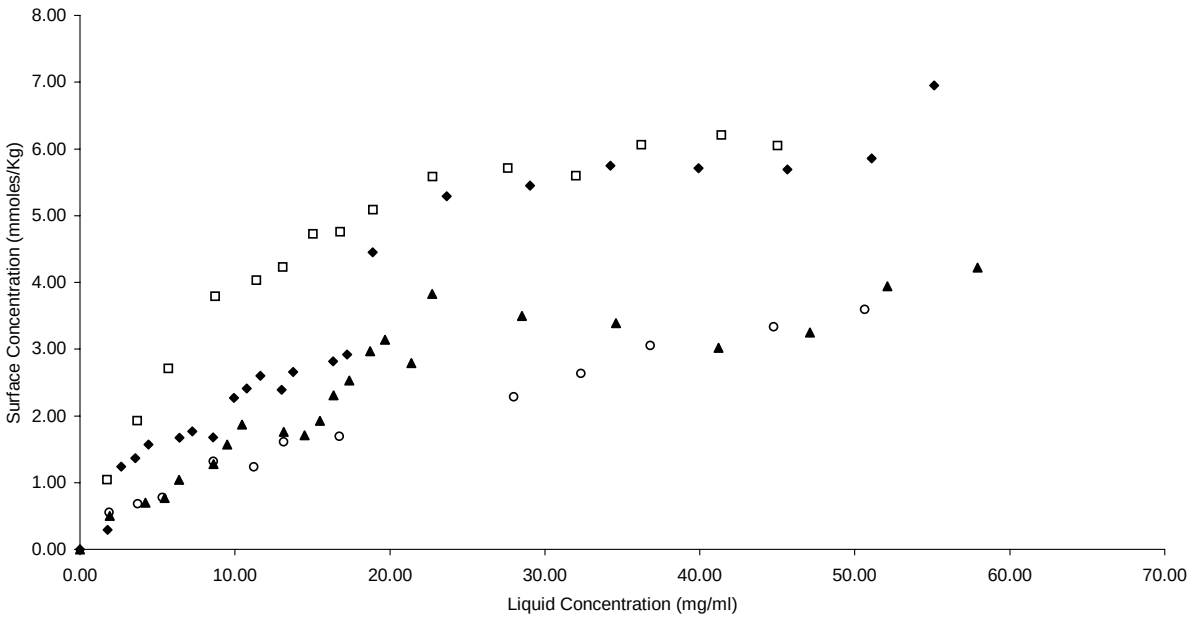

Fig. 5. Isotherms measured under batch equilibrium conditions for BSA with PPG-Sepharose in the presence of different concentrations of either $(NH_4)_2SO_4$ or Na_2SO_4 at pH 7 and 303.15 K ((▲) 1.00 M $(NH_4)_2SO_4$; (◆) 1.5 M $(NH_4)_2SO_4$; (○) 1.00 M Na_2SO_4; (□) 1.20 M Na_2SO_4) (surface concentration corresponds to mmoles of adsorbed protein per kg of wet gel).

For both salts, the protein capacity increased with the salt concentration, as expected. In comparing the isotherms, higher capacities were obtained in the presence of 1.2 M Na_2SO_4 compared to 1.5 M $(NH_4)_2SO_4$ at 303.15 K, again indicating that sodium sulfate has a greater ability to enhance hydrophobic interactions between BSA and PPG-Sepharose sorbent. However, at the lower concentration of 1.0 M, the adsorption capacity in the presence of ammonium sulfate is higher. This indicates that factors other than the release of water can significantly influence adsorption.

One possibility is that at the lower salt concentrations electrostatic effects play a role. There is some indication of the difference in electrostatic effects between the two salts in the linear data (Table 2); at 303.15 K the number of ions released in the sodium sulfate case is double that of ammonium sulfate. Another possibility is a change in the footprint of the adsorbed protein, due to a change in orientation, with salt concentration. As discussed previously [18], the distinct plateaus in the isotherms measured in the presence of ammonium sulfate indicate changes in this adsorption footprint with solution and surface conditions. The contrasting lack of plateaus for the isotherms obtained in the presence of sodium sulfate suggest that a change in orientation of BSA in ammonium sulfate case could also contribute to the generally higher capacity at 1.0 M concentration.

Calorimetric measurements of BSA adsorption on PPG-Sepharose under overloaded conditions provided valuable additional insight on the adsorption process. The FMC was operated under conditions such that the heat of adsorption is equal to the enthalpy change for adsorption. Thus, the results are reported in terms of an enthalpy change. Shown in Fig. 6 are the observed enthalpy changes of adsorption as a function of protein surface concentration at 303.15 K, pH 7.0 and different concentrations of sodium sulfate. The adsorption enthalpies (ΔH_{ads}) are all positive (endothermic process) and decrease with an increase protein adsorption.

It is useful to analyze the trends in Fig. 6 within the framework of the mechanism defined by Lin and co-workers [34–38]. They suggested that the binding mechanism in HIC can be divided into five sequential

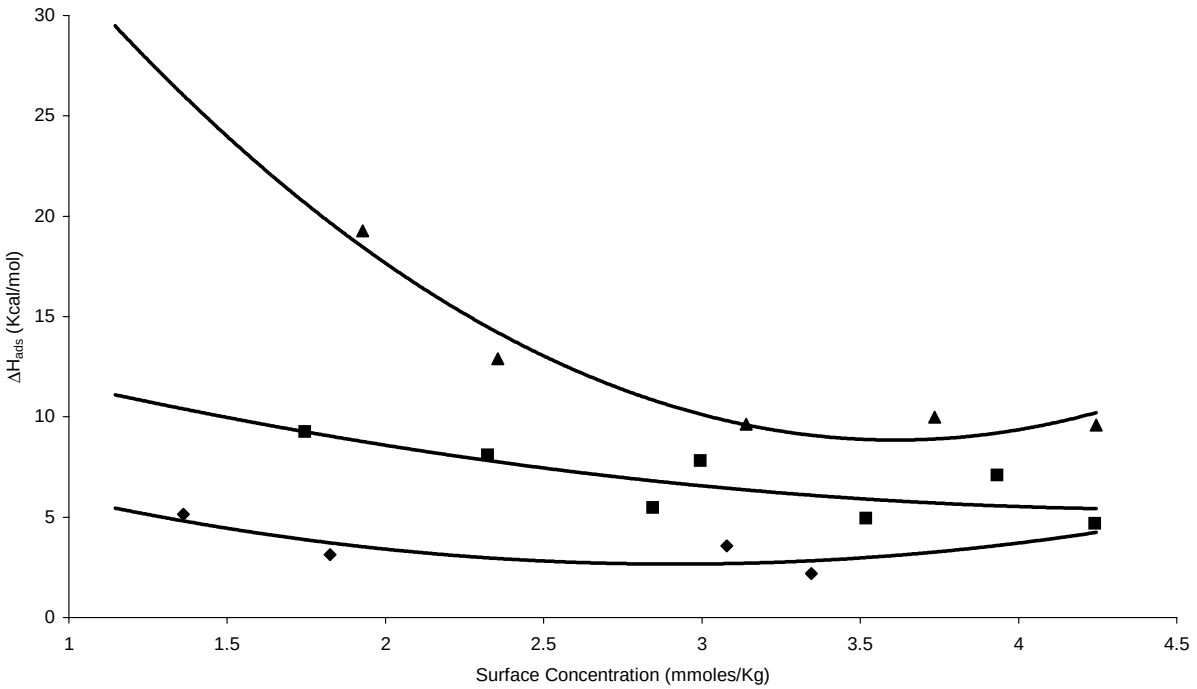

Fig. 6. Adsorption enthalpy (ΔH_{ads}) of BSA on PPG-Sepharose in the presence of different concentrations of Na_2SO_4 at pH 7.0 and 303.15 K ((◆) 0.80 M Na_2SO_4; (■) 1.00 M Na_2SO_4; (▲) 1.20 M Na_2SO_4).

sub-processes: (a) water molecules or ions surrounding the protein surface are excluded; (b) water molecules or ions surrounding the HIC sorbent are excluded; (c) hydrophobic interactions between the protein and the hydrophobic HIC sorbent; (d) structural rearrangement of the protein upon adsorption; and (e) structural rearrangement of the excluded water molecules or ions in the bulk solvent. At least two of these could underlie the observed decrease in ΔH_{ads} with increased protein coverage. These may influence behavior individually or in combination. The heat required for the dehydration of the adsorbent (sub-process (b)) may be reduced as the amount of bound protein increases. Water molecules surrounding the surface of the adsorbent are destabilized during the dehydration process, and disruption of surface water structure by initial protein adsorption may reduce energetic requirements for dehydration accompanying subsequent protein adsorption [37]. Attractive protein–protein interactions on the adsorbent surface may also be significant, and, if present, these will increase with increased protein adsorption. The magnitude of the attractive interactions could also change as a function of surface coverage due to sub-process (d). We have previously reported [17,18] that in some cases proteins re-orient on the surface as surface coverage increases, and this is accompanied by strong attractive lateral interactions between the protein molecules. Indicative of protein re-orientation is plateaus in the isotherms [18] and/or the appearance of an exothermic peak on the FMC thermogram at higher surface coverage [17,18]. Since these are not observed (Figs. 5 and 6), it appears that re-orientation of BSA is not significant in influencing protein–protein interactions.

Fig. 6 also shows that the ΔH_{ads} increases with an increase in sodium sulfate concentration. This appears to be rooted in the increase in energy required for dehydration, as a larger number of water molecules (and to a lesser extent ions) are released upon protein adsorption at higher salt concentrations. It should be noted that the influence of repulsive electrostatic interactions between adsorbed protein molecules cannot be ruled out. If these are present, shielding by the salt ions may play a role. This is, however, unlikely, since the lowest salt concentration used represents a relatively high ion density in solution, and further increases in salt concentration are not expected to enhance shielding significantly. Also, the consistent trend of a reduction in ΔH_{ads} with increased protein concentration supports the presence of attractive, rather than repulsive interactions, as was discussed earlier.

The influence of salt type on the enthalpy change of adsorption was evaluated by comparing calorimetric data at identical concentrations (1.0 M) of $(NH_4)_2SO_4$ and Na_2SO_4 at pH 7.0 and 298.15 K. The results are presented in Fig. 7. Lower values of ΔH_{ads} were obtained in the presence of $(NH_4)_2SO_4$, and, as with sodium sulfate, ΔH_{ads} decreased with an increase in protein surface concentration. The lower endothermic heat for $(NH_4)_2SO_4$ is consistent with the smaller energetic requirement for surface dehydration (of protein and adsorbent) due to the release of a smaller number of structured water molecules; the linear data (Table 2) show, on comparison of the two salts, that there is a significant difference in the number of water molecules released.

The trends observed in the enthalpy of adsorption data in this study are different from those reported by Lin and co-workers [35,38]. Using different protein/adsorbent systems from this work, they observed that the adsorption enthalpy change increased with the amount of bound protein and decreased with an increment in salt concentration. The differences could stem from the different protein/adsorbent systems studied, emphasizing the widely different behaviors that systems can manifest, and the importance of characterizing each system independently. One other possible reason for the differences is the degree of overloading. The heat of adsorption measurements were at a much higher surface coverage in this work than that of Lin and co-workers. We have previously observed for a BSA/epoxy-$(CH_2)_4$ Sepharose system [17] that at lower surface coverage the enthalpy change of adsorption initially increases with protein surface concentration, reaches a maximum and then decreases as the degree of overloading increases.

Reported in Fig. 8 is the effect of temperature on the adsorption isotherms of BSA on PPG-Sepharose gel at 1.0 M sodium sulfate (pH 7.0). The capacity is observed to increase with temperature. The equilibrium binding capacity of BSA with PPG-Sepharose is much higher at 308.15 K than at 298.15 K. The corresponding ΔH_{ads} at 303.15 and 308.15 K are presented in Fig. 9. It can be seen that the adsorptions enthalpies are larger at 308.15 K.

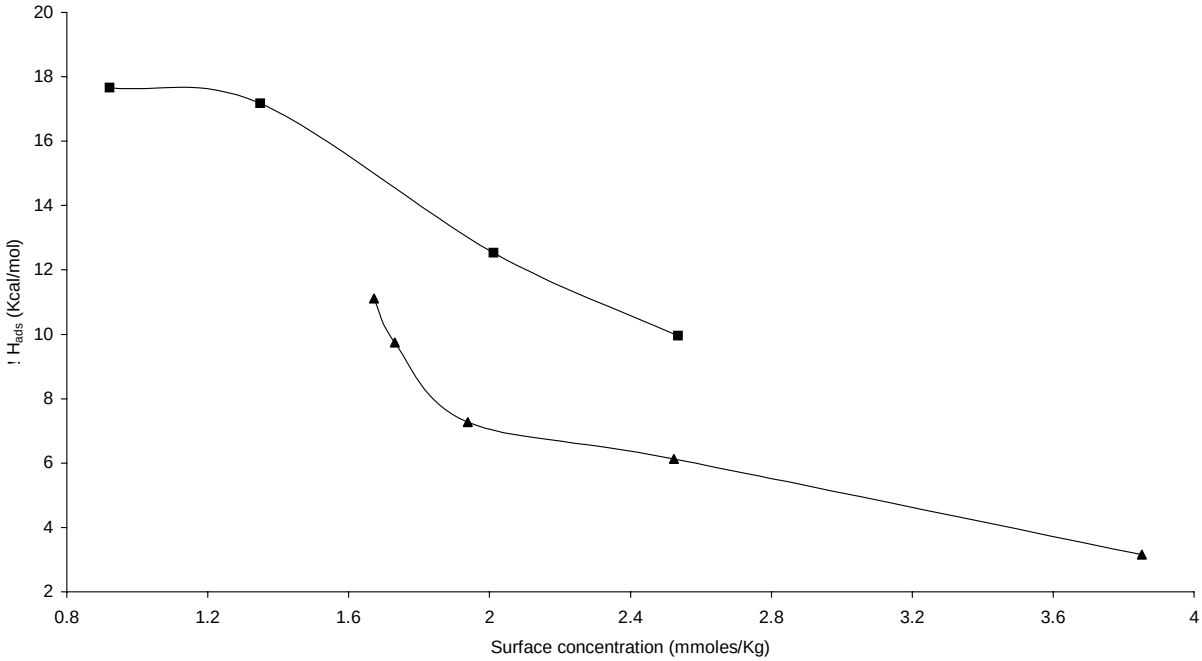

Fig. 7. Adsorption enthalpy (ΔH_{ads}) of BSA on PPG-Sepharose in the presence of different salts at pH 7.0 and 298.15 K ((▲) 1.00 M $(NH_4)_2SO_4$ and (■) 1.00 M Na_2SO_4).

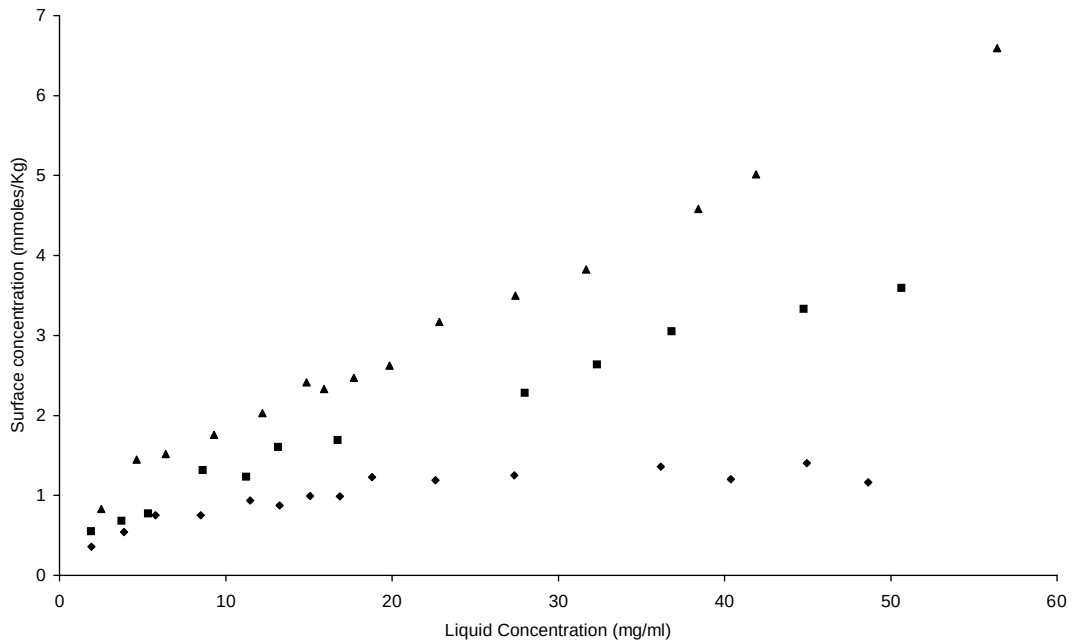

Fig. 8. Isotherms measured under batch equilibrium conditions for BSA with PPG-Sepharose in the presence of 1.0 M Na_2SO_4 at pH 7.0 and different temperatures ((◆) 298.15 K; (■) 303.15 K; (▲) 308.15 K) (surface concentration corresponds to mmoles of adsorbed protein per kg of wet gel).

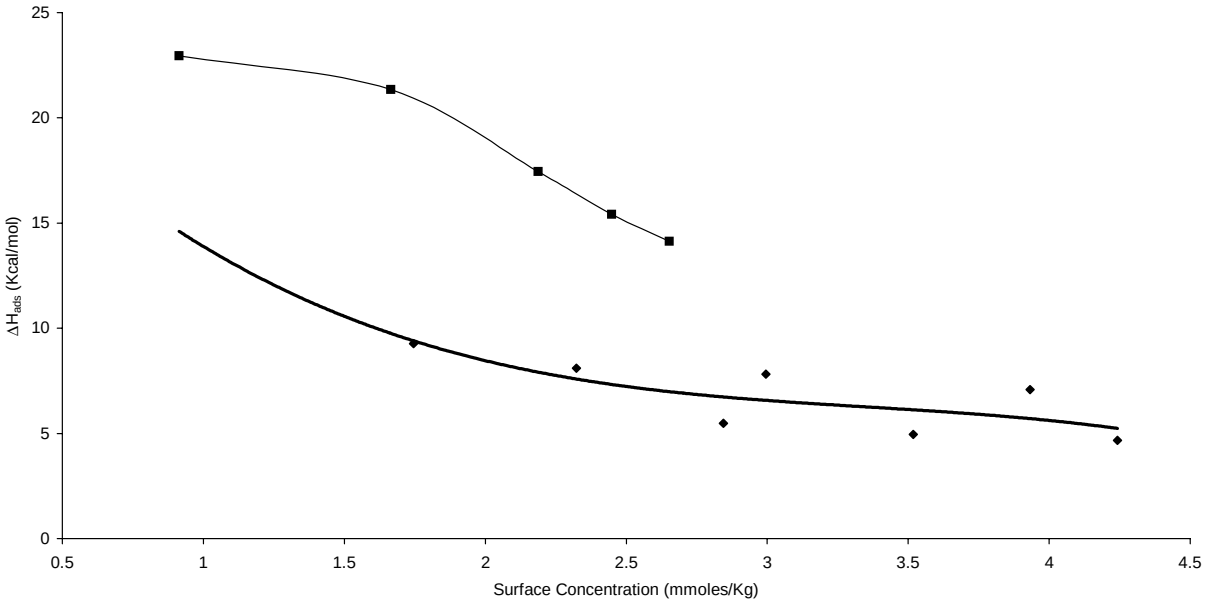

Fig. 9. Adsorption enthalpy (ΔH_{ads}) of BSA on PPG-Sepharose in the presence of 1.00 M Na_2SO_4, pH 7.0 at different temperatures ((■) Na_2SO_4 298.15 K and (◆) Na_2SO_4 308.15 K).

There are two possible reasons for the temperature dependence in Figs. 8 and 9. At higher temperatures, the number of water molecules released upon protein adsorption may be larger. However, water release estimates in Table 2 do not support such a trend, though it is recognized that the behavior in the linear region may not be representative of the non-linear region. The second possibility is a change in conformation of the protein with temperature. As was discussed earlier, a sharp change in Z value in Fig. 3 is indicative of a conformational change in the protein with temperature. Furthermore, we observed small exothermic peaks on FMC thermograms at 308.15 K. These were not present at the lower temperatures. This suggests that the conformation at the higher temperature is different.

Using the data in Figs. 8 and 9, the thermodynamic quantities ΔG_{ads}, ΔH_{ads} and ΔS_{ads} were estimated at 303.15 and 308.15 K and are shown in Table 3. ΔG_{ads} was calculated from the equilibrium binding isotherms. Using the two extreme values of ΔH_{ads} for each curve [(a) high; (b) low] in Fig. 9, the range of ΔS_{ads} was determined. As expected, ΔG_{ads} is negative. ΔG_{ads} also does not change significantly between 303 and 308 K. ΔS_{ads} is strongly positive, and increases with an increase in temperature, indicating that entropic driving force is strengthened as the temperature is increased, possibly due to a

Table 3
List of thermodynamic adsorption quantities of BSA on PPG-Sepharose using as modulator 1.00 M Na_2SO_4 at pH 7 and different temperatures

Temperature (K)	Na_2SO_4 (M)	ΔG_{ads} (kcal mol^{-1})	ΔH_{ads} (kcal mol^{-1})	ΔS_{ads} (cal mol^{-1} K^{-1})
303.15	1.0	−5.4	9.3 (a)	48.5 (a)
			4.7 (b)	33.3 (b)
308.15	1.0	−5.3	22.9 (a)	91.6 (a)
			14.1 (b)	63.0 (b)

Measured high (a) and low (b) values of adsorption enthalpy change. ΔG_{ads} was calculated from $\Delta G_{ads} = -RT\ln K$, where R is the universal gas constant, T the absolute temperature, and K the equilibrium binding constant obtained from the isotherms.

change in the conformation of the protein with temperature.

It is valuable to compare the thermodynamic parameters in Table 3 with the corresponding values obtained from linear data using the Van't Hoff analysis (Table 1). Clearly, the approximate Van't Hoff approach gives poor estimates of the thermodynamic parameters under overloaded conditions. For example, it shows no significant temperature dependence for the entropy change between 303 and 308 K, while under overloaded conditions (Table 3) a very strong dependence is observed.

4. Conclusions

The effect of salt type and concentration and the effect of temperature on the adsorption behavior of BSA on PPG-Sepharose have been studied under linear and non-linear conditions.

Analysis of data under linear conditions was accomplished with stoichiometric displacement retention model and preferential interaction approach. It has been demonstrated, using preferential interactions analysis, that the Z value (indicative of conformational changes), obtained from the stoichiometric displacement retention model, is equivalent to the number of moles of water displaced per mole of protein adsorbed. Preferential interaction analysis indicates a strong entropic driving force due to the release of a large amount of solvent on adsorption.

The adsorption of proteins under overloaded conditions was studied with heat of adsorption and isotherm measurements. The relationships between equilibrium adsorption capacity, salt concentration, salt type and temperature were evaluated. For all the conditions studied, the adsorption process was driven by an increase in entropy; all the measured heats of adsorption were endothermic. It was observed that the enthalpy change of adsorption decreased (became less endothermic) with an increase in protein adsorption, and increased at higher temperatures. The corresponding entropy change also increased with temperature. The salt concentration strongly influenced the enthalpy change of adsorption, giving higher values at higher salt concentrations. It has been argued that the trends observed indicate that protein and adsorbent surface dehydration, protein–protein interactions on the adsorbent surface, and protein re-orientation and/or conformation change all play a role in establishing the equilibrium capacity. It is therefore important to recognize that in developing a thermodynamic model for HIC adsorption, under linear and overloaded chromatographic conditions, these factors must be incorporated in addition to the primary dispersive interactions.

5. Nomenclature

$a_{\pm}$	mean ionic activity
a_i	activity of component i
a, b, c	parameters evaluated by least squares fitting for non-linear Van't Hoff analysis
C	integration constant
g	$(\partial \ln m_3/\partial \ln a_3)_{T,P}$
ΔG°	standard Gibbs free energy change associated with eluite transfer from the mobile to the stationary phase
ΔG_{ads}	Gibbs free energy change of adsorption
ΔH°	standard enthalpy change for the eluite transfer from the mobile to the stationary phase
ΔH_{ads}	enthalpy change of adsorption
I	contains a number of constants related to the affinity of a protein to the HIC column
k'	capacity factor
K	equilibrium constant
L_{d}	hydrated ligands in salt solution
m_i	molal concentration of component i
n	total number of ions
n'	number of ligands interactions with a protein molecule
R	universal gas constant
ΔS°	standard entropy change for the eluite transfer from the mobile to the stationary phase
ΔS_{ads}	entropy change of adsorption
T	temperature
Z	number of moles of water displaced per mole of protein adsorbed on the bonded phase surface

Greek letters

$\gamma_{\pm}$	activity coefficient
$\Gamma^{m}_{i,j}$	preferential interaction coefficient between species i and j in molal concentration

ν_i moles of species i in the vicinity of the protein per mole of protein
$\Delta\nu_i$ stoichiometric weighted change in the number of species in the local region of products and reactants of the process
ϕ phase ratio of a column
∂ partial derivative

Subscripts
1 water or solvent
2 protein
3 salt or solute
+ cations
− anions

Appendix A

The Z value $[\partial(\ln k')/\partial(\ln \%B)]$ proposed by Karger and co-workers [9] and the equation developed by Perkins et al. [8], both results from the application of the preferential interaction theory. By applying the two-domain model of Arakawa and Timasheff [14], a convenient interpretation of the effect of solutes on processes that can be expressed in terms of the preferential interaction coefficients is provided. For the adsorption process described by Perkins et al. [8]:

$$p\mathrm{P} + s\mathrm{S} \rightleftarrows c\mathrm{C} \tag{A.1}$$

where P is the protein, S the surface site and C the protein–surface complex. The equilibrium constant is:

$$K^m_{\mathrm{OBS}} = \frac{(m_{\mathrm{C}})^c}{(m_{\mathrm{P}})^p (m_{\mathrm{S}})^s} \tag{A.2}$$

It has been shown [13,14] that the variation of the observed equilibrium constant with the mean ionic activity of an electrolyte is [8]:

$$\left(\frac{\partial \ln K_{\mathrm{OBS}}}{\partial \ln a_{\pm}}\right)_{T,P,\mathrm{EQ}} = c(\Gamma^m_{+,\mathrm{C}} + \Gamma^m_{-,\mathrm{C}}) - p(\Gamma^m_{+,\mathrm{P}} + \Gamma^m_{-,\mathrm{P}}) - s(\Gamma^m_{+,\mathrm{S}} + \Gamma^m_{-,\mathrm{S}}) \tag{A.3}$$

Re-expressing this relationship in terms of the two-domain model yields [8]:

$$\left(\frac{\partial \ln K_{\mathrm{OBS}}}{\partial \ln a_{\pm}}\right)_{T,P,\mathrm{EQ}} = (\Delta\nu_+ + \Delta\nu_-) - \frac{nm_3}{m_1}\Delta\nu_1 \tag{A.4}$$

$\Delta\nu_i$ is the moles of i liberated by the formation of the protein–surface complex [8].

Karger and co-workers, in order to have a measurement that reflects contact area, applied, with some approximations, Eq. (A.4) to their studies. For linear chromatography, they considered $K = \phi k'$ (ϕ is the phase ratio). Since in a gradient a protein is eluted over a small salt concentration range, they assumed that the activity coefficient ($\gamma_{\pm}$) is constant ($a_3 = \varepsilon\gamma^x m_3^y$, being $y = n$ [9]). Hence, from Eq. (A.4) [9] a relationship between $\log k'$ and log salt concentration is obtained. In their studies, they founded that the slopes of the linear plots of either $\ln k'$ versus $\ln m_3$ or $\ln k'$ versus m_3 did not directly correlate with protein retention trends as a function of column temperature. However, a plot of $\ln k'$ versus $\ln \%B$ ($\%B$ is the water concentration variation in the mobile phase rather than salt concentration variation) correctly correlated retention change with temperature. Therefore, they recast Eq. (A.4) as [9]:

$$\left(\frac{\partial \ln K_{\mathrm{OBS}}}{\partial \ln a_{\mathrm{H_2O}}}\right)_{T,P,\mathrm{EQ}} = \Delta\nu_1 - \frac{m_1}{nm_3}(\Delta\nu_+ + \Delta\nu_-) \tag{A.5}$$

Assuming that the activity coefficient of water does not change over the small salt concentration range of protein elution in the gradient, they rewrote Eq. (A.5) as [9]:

$$\left(\frac{\partial \ln K_{\mathrm{OBS}}}{\partial \ln \%\mathrm{B}}\right)_{T,P,\mathrm{EQ}} = Z = \Delta\nu_1 - \frac{m_1}{nm_3}(\Delta\nu_+ + \Delta\nu_-) \tag{A.6}$$

As salts used in HIC normally reduce protein solubility, preferential hydration is going to occur. Based on this, Wu et al. assumed that the salt term on the right hand side of Eq. (A.6) is negligible relative to the water term [9]. Thus, the slope of the log–log plot, Z, is equivalent to the number of moles of water displaced per mole of protein adsorbed on the bonded phase surface [9].

The Z value obtained by Wu et al. [9] can be related to the stoichiometric displacement retention model presented by Geng et al. [10]. Taking the derivative $\partial(\ln k')/\partial(\ln \%B)$ of Eq. (1), the Z value is obtained. Thus, there is no fundamental difference between the Z values; the stoichiometric displacement retention

model does, however, break down the Z value, clarifying its contributions.

Perkins et al. [8] have rewritten Eq. (A.4) in terms of the capacity factor ($K = \phi k'$) and instead of considering the activity coefficient ($\gamma_{\pm}$) to be constant like Wu et al. [9], they incorporate the variation in the mean ionic activity with the molal salt concentration:

$$\left(\frac{\partial \ln k'}{\partial \ln m_3}\right)_{T,P,\mathrm{EQ}} = \frac{(\Delta\nu_+ + \Delta\nu_-)}{g} - \frac{nm_3}{m_1 g}\Delta\nu_1 \tag{A.7}$$

where

$$g = \left(\frac{\partial \ln m_3}{\partial \ln a_{\pm}}\right)_{T,P}.$$

Integration of Eq. (A.7) yields Eq. (4). Eq. (A.7) is a general result that can be applied to ion exchange, hydrophobic interaction or reverse phase chromatography [8]. At the salt concentrations generally used in HIC, the second term is dominant, and the increase in retention times with salt concentration is controlled by the displacement of water molecules [8], the underlying principle of the stoichiometric displacement retention model for the HIC of proteins [10].

Starting from Eq. (A.7), we can determine:

$$\frac{\partial(\ln k')}{\partial(\ln[\mathrm{H_2O}])} = \frac{\partial(\ln m_3)}{\partial(\ln[\mathrm{H_2O}])}\frac{\partial(\ln k')}{\partial(\ln m_3)} \tag{A.8}$$

By definition m_3 is the number of moles of solute (n_3) present in 1000 g water ($m_3 = (n_3 1000)/([\mathrm{H_2O}]V18)$ where V is the solution volume), thus:

$$\frac{\partial(\ln k')}{\partial(\ln[\mathrm{H_2O}])} = -\frac{\partial(\ln k')}{\partial(\ln m_3)} = \frac{nm_3}{m_1 g}\Delta\nu_1 - \frac{1}{g}(\Delta\nu_+ + \Delta\nu_-) \tag{A.9}$$

Comparing Eqs. (A.9) and (A.6) we can see that the $(nm_3)/(m_1 g)$ factor results from the incorporation of the variation in the mean ionic activity by Perkins et al. [8] in Eq. (A.4).

References

[1] J.A. Queiroz, C.T. Tomaz, J.M.S. Cabral, J. Biotechnol. 87 (2001) 143.
[2] P. Gagnon, E. Grund, T. Lindback, Biopharmaceutics April (1995) 21.
[3] M. Einarsson, L. Kaplan, E. Nordenfelt, E. Miller, J. Virol. Methods 3 (1981) 213.
[4] M.E. Thrash, N.G. Pinto, in: R.A. Myers (Eds.), Encyclopedia of Analytical Chemistry, Wiley, Chichester, 2000, p. 7259.
[5] N. Pfeiffer, Genet. Eng. News November (1995) 1.
[6] M.M. Diogo, J.A. Queiroz, G.A. Monteiro, G.N.M. Ferreira, S.A.M. Martins, D.M.F. Prazeres, Biotechnol. Bioeng. 68 (2000) 576.
[7] W.R. Melander, D. Corradini, Cs. Horváth, J. Chromatogr. 317 (1984) 67.
[8] T.W. Perkins, D.S. Mak, T.W. Root, E.N. Lightfoot, J. Chromatogr. A 766 (1997) 1.
[9] S.-L. Wu, K. Benedek, B.L. Karger, J. Chromatogr. 359 (1986) 3.
[10] X. Geng, L. Guo, J. Chang, J. Chromatogr. 507 (1990) 1.
[11] M.E. Thrash Jr., N.G. Pinto, J. Chromatogr. A 908 (2001) 293.
[12] X. Geng, Y. Shi, Sci. Chin. Ser. B 32 (1989) 11.
[13] M.T. Record Jr., C.F. Anderson, Biophys. J. 68 (1995) 786.
[14] T. Arakawa, S.N. Timasheff, Biochemistry 21 (1982) 6545.
[15] P. Rage, N.G. Pinto, J. Chromatogr. A 796 (1998) 141.
[16] A. Chandavarkar, N.G. Pinto, in: F. Meunier (Ed.), Fundamentals of Adsorption, Elsevier, Amsterdam, 1998, p. 413.
[17] M.A. Esquibel-King, A.C. Dias-Cabral, J.A. Queiroz, N.G. Pinto, J. Chromatogr. A 865 (1999) 111.
[18] A.C. Dias-Cabral, N.G. Pinto, J.A. Queiroz, Sep. Sci. Technol. 37 (2002) 1505.
[19] M.E. Thrash Jr., N.G. Pinto, J. Chromatogr. A 944 (2002) 61.
[20] L. Sundberg, J. Porath, J. Chromatogr. 90 (1974) 87.
[21] M.M. Diogo, S. Silva, J.M.S. Cabral, J.A. Queiroz, J. Chromatogr. A 849 (1999) 413.
[22] K. Kandori, M. Mukai, A. Fujiwara, T. Ishikawa, J. Colloid Interface Sci. 212 (1999) 600.
[23] R.E. Shansky, S.-L. Wu, A. Figueroa, B.L. Karger, in: K.M. Gooding, F.E. Regnier (Eds.), HPLC of Biological Macromolecules: Methods and Applications, Marcel Dekker New York, 1990, p. 95.
[24] S. Pahlman, J. Rosengren, S. Hjertén, J. Chromatogr. 131 (1977) 99.
[25] W. Melander, Cs. Horváth, Arch. Biochem. Biophys. 183 (1977) 200.
[26] A. Vailaya, Cs. Horváth, Ind. Eng. Chem. Res. 35 (1996) 2964.
[27] D. Haidacher, A. Vailaya, Cs. Horváth, Proc. Natl. Acad. Sci. U.S.A. 93 (1996) 2290.
[28] D.W. Lee, B.Y. Cho, Bull. Korean Chem. Soc. 14 (1993) 515.
[29] R.H. Ingraham, S.Y.M. Lau, A.K. Taneja, R.S. Hodges, J. Chromatogr. 327 (1985) 77.
[30] E.S. Parente, D.B. Wetlaufer, J. Chromatogr. 288 (1984) 389.
[31] K. Benedek, S. Dong, B.L. Karger, J. Chromatogr. 317 (1984) 227.

[32] Table Curve 2D, "Automated Curve Fitting Software", version 2.0, Jandel Scientific, AISN Software, 1989–1994.
[33] M.P. Deutscher, Methods Enzymol. 182 (1990) 409.
[34] W. Norde, Adv. Colloid Interface Sci. 25 (1986) 267.
[35] F.-Y. Lin, W.-Y. Chen, M.T.W. Hearn, Anal. Chem. 73 (2001) 3875.
[36] H.-M. Huang, F.-Y. Lin, W.-Y. Chen, R.-C. Ruaan, J. Colloid Interface Sci. 229 (2000) 600.
[37] F.-Y. Lin, W.-Y. Chen, R.-C. Ruaan, H.-M. Huang, J. Chromatogr. A 872 (2000) 37.
[38] Y.-S. Tsai, F.-Y. Lin, W.-Y. Chen, C.-C. Lin, Colloids Surf. A 197 (2002) 111.